

# Characteristics of Friction Behavior of Ceramic Friction Materials according to Surface Materials

Ji-Hun Park<sup>1</sup> · Jung-Woo Lee<sup>2\*</sup> · Jong-Won Kwark<sup>3</sup> · Woo-Jin Han<sup>4</sup> · Oneil Han<sup>5</sup>

(Received November 30, 2023 / Revised December 21, 2023 / Accepted December 22, 2023)

Friction material, an integral constituent of bearing supports, facilitates frictional interactions between two components. Polytetrafluoroethylene (PTFE), a commonly employed friction material in bearing supports, has assessed resultant friction equilibrium. Nonetheless, protracted utilization diminishes frictional performance as the lubricating agent is progressively depleted. Friction materials can affect the entire structural system. Hence, this study applied ceramic material as a friction material due to its high strength, low friction, and low deformation. The frictional behavior was investigated using a cyclic friction test, considering various friction materials as the primary design variables and examining their covariance in cyclic frictional movements. The results substantiated that the ceramic friction material yielded a low variance and friction coefficients in cyclic frictional movements.

**Keywords :** Ceramic, Friction material, Friction behavior, Statistical analysis, Sliding plate, Bridge support

## 1. Introduction

Bearing support plays a pivotal role in retaining structural performance, prompting various investigations aimed at enhancing their mechanical and chemical attributes. Numerous studies (Yang et al. 2021; Adamov et al. 2022; Wei et al. 2020; Lee et al. 2017; Han et al. 2023) have proposed novel friction materials crucial for maintaining a low-friction state between two members. The friction material shown in Fig. 1, must exhibit a low friction coefficient to accommodate horizontal and rotational movements under external forces, such as vehicle, temperature, and wind loads (Joh et al. 2006). The longevity of a bridge, typically estimated at approximately 50 yr, hinges on the performance of this friction material. However, the durability of an existing spherical bearing

support is approximately 5 yr, approximately 1/10 of the lifespan of the bridge. The durability period signifies the interval until defects manifest, while the standard replacement cycle for conventional bridge support is approximately 15 yr. Any damage to the friction material can degrade the performance of the structures. The entire bearing support must be replaced in such instances because the friction material cannot be replaced separately. Consequently, it translates into increased maintenance and life-cycle costs for the structures.

The early support bearing featured a robust spherical brass bearing support, wherein nonfueled lubricants such as graphite and molybdenum were incorporated within a high-power brass matrix. Nonetheless, challenges arose in the form of fluctuations linked to copper prices, impacting the cost of the bearing support. Furthermore, the prolonged usage

\* Corresponding author E-mail: [duckhawk@kict.re.kr](mailto:duckhawk@kict.re.kr)

<sup>1</sup>Researcher, Department of Structural Engineering Research, Korea Institute of Civil Engineering and Building Technology, Gyeonggi-do, 10223, Republic of Korea

<sup>2</sup>Senior Researcher, Department of Structural Engineering Research, Korea Institute of Civil Engineering and Building Technology, Gyeonggi-do, 10223, Republic of Korea

<sup>3</sup>Senior Research Fellow, Department of Structural Engineering Research, Korea Institute of Civil Engineering and Building Technology, Gyeonggi-do, 10223, Republic of Korea

<sup>4</sup>Senior Research Engineer, Esco RTS Co., Ltd., Esco Building, Seoul, 06134, Republic of Korea

<sup>5</sup>Manager, Hyundai Engineering & Construction, Hyundai Building, Seoul, 03058, Republic of Korea

Copyright © 2023 by Korean Recycled Construction Resources Institute

This is an Open-Access article distributed under the terms of the Creative Commons Attribution Non-Commercial License (<http://creativecommons.org/licenses/by-nc/3.0>) which permits unrestricted non-commercial use, distribution, and reproduction in any medium, provided the original work is properly cited

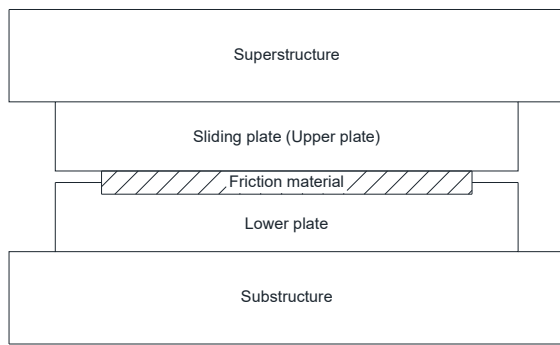


**Fig. 1. Configuration of bearing support (schematic diagram)**



**(a) high-strength brass friction material rust**      **(b) corrosion of bearing supports due to rust**

**Fig. 2. Corrosion of bearing supports**

led to a decline in the performance of the friction material. Particularly, integration due to gradual rust generation is problematic because this support type involves contact between two metal surfaces(Fig. 2).

Current friction materials used in most bearing supports are engineering plastic (EP), ultra-high molecular weight polyethylene (UHMWPE), and polytetrafluoroethylene (PTFE) (Choi et al, 2019; Dong et al, 2011; Kamenskih and Trufanov 2013; Pavlenko et al, 2013). These materials consist of inorganic compounds, with the principal constituent being fluororesin. Oh et al.(2013) applied PTFE to common bearing supports for a 40 m simple span and a two-span continuous bridge. However, PTFE is susceptible to tearing and deformation over prolonged usage, prompting the widespread adoption of UHMWPE and EP owing to their excellent properties and high durability. They offer enhanced durability and permissible bearing resistance. The long-term friction test demonstrated that the sliding distance of EP was 2-5 times longer than that of PTFE(Oh et al, 2016). However, they exhibited a threefold higher friction coefficient than that of PTFE. Lubrication is employed to ensure smooth structural

behavior(Wang et al, 2021; Mnif et al, 2013; Zhang et al, 2015; Feng et al, 2019; Oh et al, 2015). However, the lubrication performance of the friction materials decreases as structures remain in service for extended periods owing to the lubricant depletion or deformation of the friction materials.

Recently, the frictional behavior of bearing supports has been degraded owing to the corrosion and deformation of friction materials resulting from long-term use. This deterioration has led to issues concerning the structural behavior of the entire bridge. Ceramics exhibit resistance to deformation and corrosion owing to their inherent properties. Additionally, their surface roughness can be adjusted to suit the specific requirements. These advantages offer potential solutions to address challenges associated with the high deformation and corrosion of conventional friction materials, ensuring the efficacy of bridge supports. A study has investigated the possibility of incorporating ceramics into friction materials. Ceramic friction materials represent promising alternatives to mitigate the shortcomings of existing friction materials, chiefly characterized by and have reduced susceptibility to corrosion and deformation. This study investigated the possibility of using ceramic friction materials by combining them with various other materials. Furthermore, the variability in the friction coefficient according to the cyclic frictional behavior of the ceramic friction material was analyzed per the AASHTO standards(ASSHTO 2010).

## 2. Frictional behavior tests with friction materials

### 2.1 Test setup

This test was based on the friction test method outlined by Han et al.(2023). The friction tests adhered to the AASHTO standard, which describes a method for evaluating the effect of frictional behavior on the bearing support. The friction test machine, capable of measuring displacement and load acting upon the specimens, is shown in Fig. 3. Detailed specifications of the test machines are listed in Table 1. The friction material specimen was configured with a thickness and diameter of 5

mm and 76 mm (3 in), respectively, per the guidelines set forth by the AASHTO standard(Fig. 4). The friction material was attached to the bearing jig of the vertical actuator and surmounted using a sliding plate. During the friction test, a vertical load was applied, followed by applying a horizontal load under displacement control, maintained at a velocity of 1 mm/s. The one-sided horizontal frictional distance was

spanned 10 mm and was repeated 20 times in both directions (+, -).

### 2.2 Material properties

The ceramic and stainless steel(Specifications 2010) used in the specimens and sliding plates, respectively, were investigated using a mill test. Particularly, ceramics comprised zirconia( $ZrO_2$ ), which exhibits the highest compressive strength and satisfies low-friction conditions. The results are summarized in Table 2 and 3. The Young's modulus for the ceramic and stainless steel were approximately identical, measuring 220 GPa and 210 GPa, respectively. The Poisson's ratios for both materials were equivalent, at 0.297 and 0.3, respectively. Additionally, the ceramic demonstrated a compressive strength of 3,997 MPa, while the stainless steel exhibited a tensile strength of 656 MPa. The hardness values of the ceramic and stainless steel, as determined by the Vickers hardness testing, were 1,100 and 500, respectively. Furthermore, the ceramic exhibited a roughness of 0.8(Standard PN-EN ISO 4288 1997; Frantsen and Mathiesen 2009).



Fig. 3. Friction test setup

Table 1. Friction test machine specifications

Technical specification	Value
Maximum vertical load	100 kN
Maximum vertical loading rate	100 mm/s
Maximum vertical stroke	±100 mm
Maximum horizontal load	50 kN
Maximum horizontal loading rate	100 mm/s
Maximum horizontal stroke	±100 mm

Table 2. Material properties

Specification	Ceramic	Stainless-steel
Young's modulus (GPa)	220	210
Compressive/tensile strength (MPa)	3,997	656
Poisson's ratio	0.297	0.3
Hardness (vickers hardness)	1,100	152
Roughness	0.8	0.8

Table 3. Proportions of ceramic

Element	Composition (%)
$ZrO_2$	94.66
$Y_2O_3$	5.34
$Al_2O_3$	0.23
$Fe_2O_3$	0.001
$TiO_2$	0.001
$SiO_2$	0.004
$CaO$	0.001
$Na_2O$	0.003

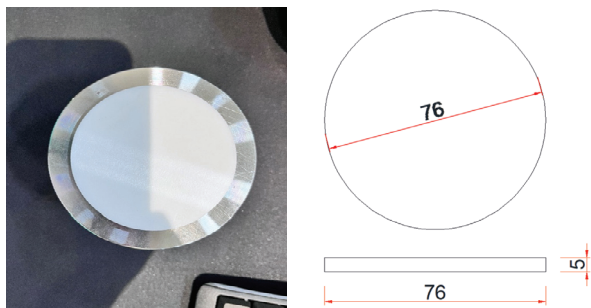


Fig. 4. Friction material

### 2.3 Test plan

The test plan considered the differences in the material type concerning the friction surface and vertical loads. The vertical load capacities ranged from 10 to 90 kN in ceramic-ceramic-type tests to evaluate the effect of vertical loads. A detailed plan is presented in Table 4. Nomination refers to the material names and vertical loads of each specimen.

**Table 4. Test plan for evaluating friction material**

Test	Friction material	Sliding plate	Vertical load (kN)
C-S-10	Ceramic	Stainless steel	10
S-C-10	Stainless steel	Ceramic	10
C-C-10	Ceramic	Ceramic	10
C-C-30	Ceramic	Ceramic	30
C-C-50	Ceramic	Ceramic	50
C-C-90	Ceramic	Ceramic	90

### 3. Friction test results and analysis

Fig. 5 shows the results of the friction experiment on the friction material as a horizontal load-displacement graph. The average friction coefficient was calculated using Equation 1 by averaging the maximum horizontal load values attained during each cycle of every test. Subsequently, the degree of dispersion according to the repeated load was evaluated, and the findings are summarized in Table 5.

$$\mu = \frac{F_h}{F_v} \tag{1}$$

where  $\mu$  is the friction coefficient,  $F_h$  is the horizontal force, and  $F_v$  is the vertical force.

**Table 5. Test results**

Test	Vertical load (kN)	Friction coefficient	Covariance (COV)
C-S-10	10	0.40	0.105
S-C-10	10	0.41	0.064
C-C-10	10	0.17	0.079
C-C-30	30	0.15	0.071
C-C-50	50	0.18	0.092
C-C-90	90	0.20	0.052

### 3.1 Effect of friction according to materials

A comparative analysis of the friction coefficients across different materials was conducted using C-S-10, S-C-10, and C-C-10. In the case of C-S-10 and S-C-10, the average friction coefficients were 0.40 and 0.41, respectively. The COV for these tests were 0.105 and 0.064, respectively, indicating a relatively large variation of approximately 4 %. This variation can be attributed to the hardness of the ceramic being larger than that of the stainless steel, causing the friction material to penetrate the mirror slide during the horizontal movement in the C-S-10 experiment, resulting in a higher evaluation of horizontal load. Conversely, the average friction coefficient in the case of C-C-10 was less than half that observed in the other tests. We note that the relatively larger COV in this case was influenced by the difference in the fine load when a lower friction load occurred than the two aforementioned tests. The friction between the ceramics was lower than between the ceramic and stainless steel.

### 3.2 Effect of friction according to vertical loads

Evaluating the friction surface interactions among ceramics involved examining changes in the friction coefficient at load levels of 10, 30, 50, and 90 kN. Across each load increment, the average friction coefficient consistently ranged from 0.15 to 0.20, with a difference of approximately 5 %. In the case of the COV, it decreased gradually as the capacity of the vertical load increased. This trend became particularly pronounced when the load reached 90 kN, where the COV approached approximately 5 %. We found that the contact force of the friction surface increased as the vertical load increased, stabilizing the friction behavior.

A bearing supports is a structure that is subjected to a very large constant compression force due to the self-weight and dead load of the superstructure. Although the magnitude of the compressive force varies from moment to moment due to external fluctuating loads, it is a very small load compared to the compressive force that is always reloaded, and the fluctuation is also very small. In addition, even if shocks and vibrations occur, the energy is gradually dissipated and

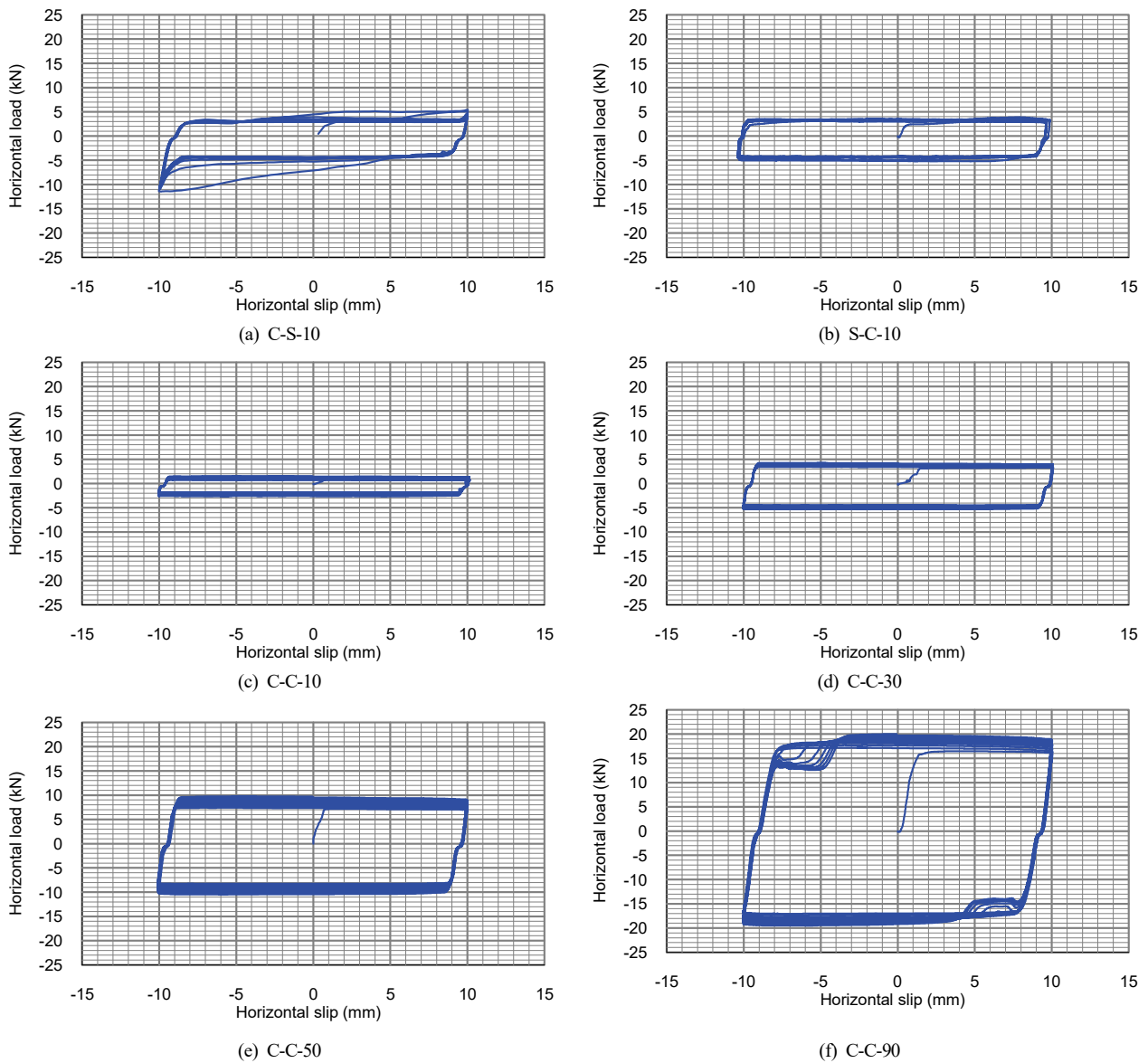


Fig. 5. Horizontal load-slip curve (friction load)

attenuated before it is transmitted to the ceramic friction material, and although ceramic materials are brittle, it is considered that shocks and vibrations do not need to be considered.

#### 4. Evaluation of frictional behavior under actual condition

A series of 100 repetitive friction tests were conducted by applying a vertical load of 15 MPa to the friction material to

simulate real-world operating conditions. This 15 MPa stress level aligns with the vertical stress encountered in the bridge support typically used in general girder bridges. The analysis centered on examining friction behavior under load conditions. Fig. 6 presents the horizontal load-displacement curve and capacity of the horizontal friction load over time. The friction load exhibited remarkable consistency within the horizontal load-displacement curve. The evaluation of the friction coefficient revealed an average value of 0.17, with a COV of approximately 0.031. Given the consistent friction load

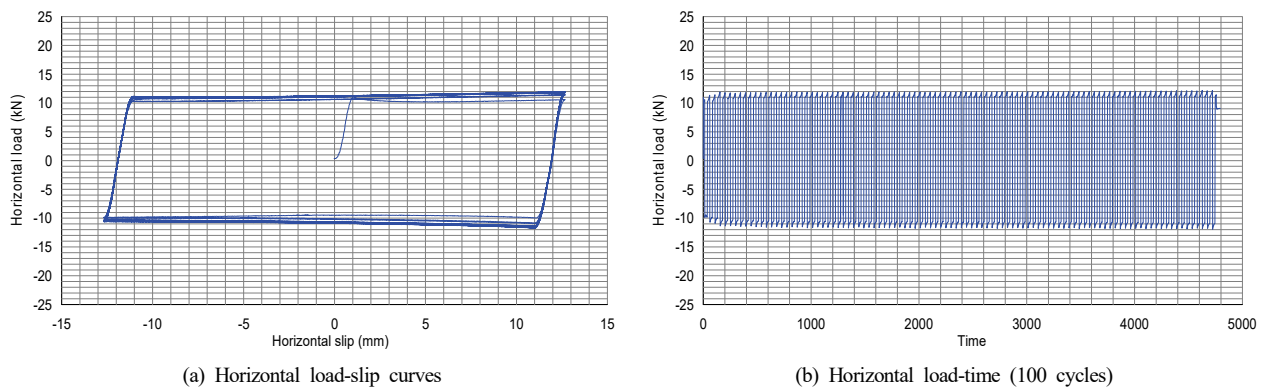


**Fig. 6. Friction test results with both ceramic-friction materials (under 15 MPa of vertical load)**

observed with only a minor 3 % variation and the stable friction coefficient of 0,17, including ceramics in the composition of friction materials and sliding plates is believed to engender stable friction behavior.

## 5. Conclusion

This study analyzed the friction behavior of the material through a friction test. Moreover, it assessed the reliability of the friction behavior of the ceramic friction material under varying vertical load magnitudes, with a specific focus on the 15 MPa vertical load, representative of the actual bridge conditions. The following conclusions were drawn based on the experimental findings:

1. The utilization of both ceramic and stainless steel materials yielded a similar friction coefficient, approximately at 0,40 level, regardless of the combination of friction material and sliding plate. However, a friction coefficient of 0,20 or lower is required. Consequently, this material combination may not be suitable for such purposes.
2. In instances where ceramic materials were employed for both friction materials and sliding plates, the average friction coefficient remained consistent at approximately 0,17, irrespective of variations in vertical load magnitude. However, the variation in the friction coefficient decreased with increasing the magnitude of the vertical load, indicating a high level of reliability in friction

behavior.

3. When subjected to a vertical load of 15 MPa, akin to real-world bridge support conditions, and repeated 100 times, the friction coefficient remained at 0,17, consistent with evaluating the friction coefficient under varying loads. Notable, the COV remained exceptionally low, at approximately 3 %. Consequently, the feasibility of the ceramic friction materials in bridge supports was affirmed.
4. The ceramics used in this study exhibited a roughness coefficient of 0,8, which may yield a relatively high friction coefficient. Further research is warranted to explore whether a low friction coefficient can be achieved by setting a low illumination coefficient through subsequent studies.

## Conflicts of interest

None.

## Acknowledgments

This study was conducted under the KICT Research Program (project no. 20230136-001, Development of sliding pads for bridge bearings with improved durability using ceramics) funded by the Ministry of Science and ICT.

## References

- AASHTO, B.D.S. (2010). American Association of State Highway and Transportation Officials, Washington, DC, 4.
- Adamov, A.A., Kamenskikh, A.A., Pankova, A.P. (2022). Influence analysis of the antifriction layer materials and thickness on the contact interaction of spherical bearings elements, *Lubricants*, **10(2)**, 30.
- Choi, E., Choi, Y., Lee, J., Jang, Y., Lee, S. (2019). Assessment of friction of ep frictional materials used for spherical bearings of railway bridges, *Journal of Korean Society of Steel Construction*, **31(4)**, 293–299 [in Korean].
- Dong, S., Chung, K.H., Lee, K.S. (2011). Effect of surface roughness of counterface on tribological characteristics of PTFE and UHMWPE, *Tribology and Lubricants*, **27(6)**, 293–301 [in Korean].
- Frantsen, J.E., Mathiesen, T. (2009). Specifying stainless steel surfaces for the brewery, dairy and pharmaceutical sectors, *Nace Corrosion*, NACE–09373.
- Feng, C., Zhang, D., Chen, K. (2019). In situ microscopic observations of dynamic viscoelastic contact and deformation at a friction interface, *Materials Express*, **9(3)**, 235–244.
- Han, O., Kwark, J.W., Lee, J.W., Han, W.J. (2023). Analytical study on the frictional behavior of sliding surfaces depending on ceramic friction materials, *Applied Sciences*, **13(1)**, 234.
- Joh, C., Yoon, H., Kim, Y.J. (2006). Accumulated sliding distance of the sliding element in the bridge bearing, *Korean Society of Civil Engineers*, 1320–1323.
- Kamenskikh, A.A., Trufanov, N.A. (2013). Numerical analysis of the stress state of a spherical contact system with an interlayer of antifriction material, *Comput. Contin. Mech*, **6**, 54–61.
- Lee, K.H., Park, D.B., Jang, K.S., Sim, K.C., Choi, J.S. (2017). Evaluate the friction coefficient of friction pendulum bearing applied new friction material, *Korean Society of Civil Engineers*, 1353–1354.
- Mnif, R., Ben Jemaa, M.C., Kacem, N.H., Elleuch, R. (2013). Impact of viscoelasticity on the tribological behavior of PTFE composites for valve seals application, *Tribology transactions*, **56(5)**, 879–886.
- Oh, S.T., Lee, D.J., Yeon, J.S., Lee, H.J., Jeong, S.H. (2013). Dynamic behaviors of bearings of the two-span continuous PSC box bridge with 40 m span for KTX vehicle, *Proceedings of the 25th Annual Conference, The Korean Society for Railway*, 130–132 [in Korean].
- Oh, J., Jang, C., Kim, J.H. (2015). A study on the characteristics of bridge bearings behavior by finite element analysis and model test, *Journal of Vibroengineering*, **17(5)**, 2559–2571.
- Oh, S.T., Lee, D.J., Jun, S.M., Jeong, S.H. (2016). A long-term friction test of bridge bearings considering running speed of next generation train, *Journal of the Korea Institute for Structural Maintenance and Inspection*, **20(2)**, 34–39 [in Korean].
- Pavlenko, V.I., Bondarenko, G.G., Tarasov, D.G., Edamenko, O.D. (2013). Gamma modification of radiation-resistant fluoroplastic composite, *Inorganic Materials: Applied Research*, **4**, 389–393.
- Standard PN-EN ISO 4288. (1997). Geometrical Product Specifications (GPS)-Surface Texture: Profile Method-Rules and Procedures for the Assessment of Surface Texture.
- Specifications, K.H.B. (2010). Korean Ministry of Construction and Transportation.
- Wei, W., Yuan, Y., Igarashi, A., Zhu, H., Luo, K. (2020). Generalized hyper-viscoelastic modeling and experimental characterization of unfilled and carbon black filled natural rubber for civil structural applications, *Construction and Building Materials*, **253**, 119211.
- Wang, H., Sun, A., Qi, X., Dong, Y., Fan, B. (2021). Experimental and analytical investigations on tribological properties of PTFE/AP composites, *Polymers*, **13(24)**, 4295.
- Yang, Y., Zhang, Y., Ju, J. (2021). Study on the mechanical properties of a type of spherical bearing, *Journal of Theoretical and Applied Mechanics*, **59(4)**, 539–550.
- Zhang, Y., Xu, S., Zhang, Q., Zhou, Y. (2015). Experimental and theoretical research on the stress-relaxation behaviors of PTFE coated fabrics under different temperatures, *Advances in Materials Science and Engineering*, **2015**, 319473.